Thermochimica Acta, 174 (1991) 115–130
Elsevier Science Publishers B.V., Amsterdam

PHASE DIAGRAMS AND CRYSTAL GROWTH OF OXIDE SUPERCONDUCTORS

HANS J. SCHEEL

Institute for Micro- and Optoelectronics, Physics Department, Swiss Federal Institute of Technology, CH-1015 Lausanne (Switzerland)

F. LICCI

MASPEC Institute of C.N.R., I-43100 Parma (Italy)

(Received 18 May 1989)

ABSTRACT

Phase-diagram data for the cuprate superconductors have become available only slowly owing to specific problems such as sluggish equilibration reactions. The phase relations of the system Y_2O_3–BaO–CuO_x show that only $BaCuO_2$–CuO melts can be used as solvents for the crystal growth of YBCO from high-temperature solutions. Data on the Bi- and Tl-cuprate superconductors are not available. The system $(La,Sr)_2CuO_4$–CuO_x indicates a simple eutectic and high solubility of the superconductor, which therefore can be grown as large crystals.

INTRODUCTION

The discovery of superconductivity above the boiling point of liquid nitrogen (at 77 K) in $YBa_2Cu_3O_{7-x}$ (YBCO), in Bi–Ca–Sr-cuprates (abbreviated as Bi-cuprates) and in Tl–Ca–Ba-cuprates (Tl-cuprates) initiated a need for chemically and structurally single-phase ceramics with high current densities, for high-quality single crystals, and for epitaxial single-crystal layers of these compounds. However, owing to thermal and chemical instabilities of these cuprates, materials of the required quality have not yet been prepared. Major obstacles are insufficient availability of reliable phase equilibrium data for YBCO, and non-availability of phase data for the Bi- and Tl-compounds. The phase diagrams are needed for optimized planning of crystal growth experiments, for achieving large crystals, for estimating the temperature programs for maximum stable growth rates in order to obtain inclusion-free crystals [1], and for analysis of segregation problems in order to achieve crystals of the desired composition and homogeneity [2].

An attempt is made here to review and discuss the available data on the phase diagram of YBCO–$BaCuO_2$–CuO_x and the primary crystallization field of YBCO for crystal growth and epitaxial film deposition from high-temperature solutions. The discussion of specific aspects of the system Y_2O_3–BaO–CuO_x is followed by crystal growth of YBCO utilizing these data. In the case of the lower-T_c cuprate superconductor $La_{1.85}Sr_{0.15}CuO_4$ the phase relations are less complex than for YBCO: owing to the increased thermal stability of La–Sr-cuprate and its high solubility in CuO_x melts, large crystals could be grown by a few groups. Finally, the scarce data on the Bi- and Tl-cuprate superconductors will be presented and followed by conclusions.

EXPERIMENTAL ASPECTS AND PROBLEMS IN DETERMINING PHASE DIAGRAMS OF RARE-EARTH AND ALKALINE-EARTH CUPRATES

The determination of the pseudo-ternary systems consisting of very high-melting rare-earth oxides (e.g. for Y_2O_3, $T_m = 2400\,^\circ C$) and alkaline-earth oxides (e.g. for BaO $T_m = 1900\,^\circ C$), and the relatively low-melting CuO_x ($T_m = 1140\,^\circ C$ in air) is complex, for the several reasons given below.

(1) The large differences in melting point of the oxides mentioned above and of high-melting compounds such as $Ba_3Y_4O_9$ (2160 °C) on the one hand and of low-melting eutectics (e.g. 825 °C for the CuO–Cu_2O–$BaCuO_2$–$BaCu_2O_2$ eutectic) on the other hand.

(2) Very slow equilibration at a given temperature with the actual oxygen partial pressure leading to the presence of non-equilibrium solid and liquid phases.

(3) Sluggish reactions typical for peritectic systems, such as slow dissolution of high-temperature phases (once formed) and reaction layers around components which ought to participate in equilibration.

(4) The complexity of the system "requiring the preparation of hundreds of compositions and ten times that number of individual experiments" [3].

(5) A specific problem is, in the case of YBCO, the interaction of the corrosive Ba–Cu–O melts with commercial crucible materials: Pt is heavily wetted and attacked. It forms Ba–Pt–O compounds or Pt-containing phases such as $Y_2Ba_2CuPtO_8$ [4] and $Y_2Ba_3Cu_2PtO_9$ [5,6]. Alumina is corroded and leads to incorporation of 0.5 to 3 at.% Al in YBCO and, at extended times above 950 °C, to the formation of aluminate phases [7,8]. Corrosion studies [7] of alumina, zirconia and of tin oxide revealed a common corrosion mechanism with the sequence (a) diffusion, (b) reaction layer, and (c) dissolution. This suggests a search for novel crucible materials. The strong wetting of Ba-cuprate melts may lead to excessive creep, so that the liquid may leave the crucible and creep along the thermocouples. This generally

leads to the necessity of replacing the DTA measuring head. The least corroded crucible materials seem to be thoria [9] and MgO single crystals [3].

As a consequence of the above problems there are numerous factors which have to be taken into account in a comprehensive study of the cuprate superconductor phase diagrams. Dynamic methods of analysis such as DTA and (simultaneous) TG have to be complemented by static long-time annealing and quenching experiments and by a careful examination of reversible reactions. Separation of solid and liquid phases by creep or merely by gravitation has to be avoided by intensive mixing and densification of the starting mixtures and by sufficiently slow heating rates. Differences between first and successive DTA runs indicate problems which have to be analyzed. X-ray analysis of reaction products with at least 1% sensitivity needs to be carried out, for instance by taking long-exposure Guinier photographs or by using high-quality diffractometers [10]. X-ray identification of all diffraction lines may be combined with microscopic (petrographic) phase analysis and structural/chemical investigations by means of a scanning electron microscope with attached energy-dispersive X-ray fluorescence analysis. By a combination of these characterization techniques, reliable data can be obtained; however, they require a large and time-consuming effort in view of the complexity of the multi-component cuprate systems.

$BaO-CuO_x$

From the binary systems of the three oxides BaO, Y_2O_3 and CuO_x, the phase diagram $BaO-CuO_x$ is of interest to the crystal grower because of the application of $BaO-CuO_x$ melts as solvents for growth of YBCO. The phase diagram of this system has been published by Roth et al. [3] and by Nevřiva et al. [11]. The reported eutectic compositions varied between 18 mol% BaO [12], 22.2 mol% [13], 28 mol% [11,14], 33.3 mol% [15] to 40 mol% [3,16]. Reported eutectic temperatures lie in the ranges 895 ± 5 °C for air [3,16] and 925–950 °C for an oxygen atmosphere [11,15,16]. Reported temperatures below 880 °C [12–14] indicate the presence of non-equilibrium phases such as Cu_2O and $BaCu_2O_2$ [17,18]. From the work of Oka et al. [19] the eutectic data of about 30 mol% BaO/70 mol% CuO and 910–920 °C can be deduced. Our own systematic experiments [20] yielded eutectic compositions of 29,5 ± 1 mol% BaO in air and 33 ± 3 mol% in oxygen, thus confirming one of the earlier values [15]. The eutectic temperatures from the first DTA heating curves are 930 ± 10 °C in oxygen and 915 ± 10 °C in air. The equilibrium eutectic temperatures in air may be about 10–20 °C lower, and would then correspond to the value of 895 °C given above. Also, the crystallization and flux separation experiments [20] gave a eutectic temperature of 900 ± 10 °C in air. After oxygen loss and first melting, the successive

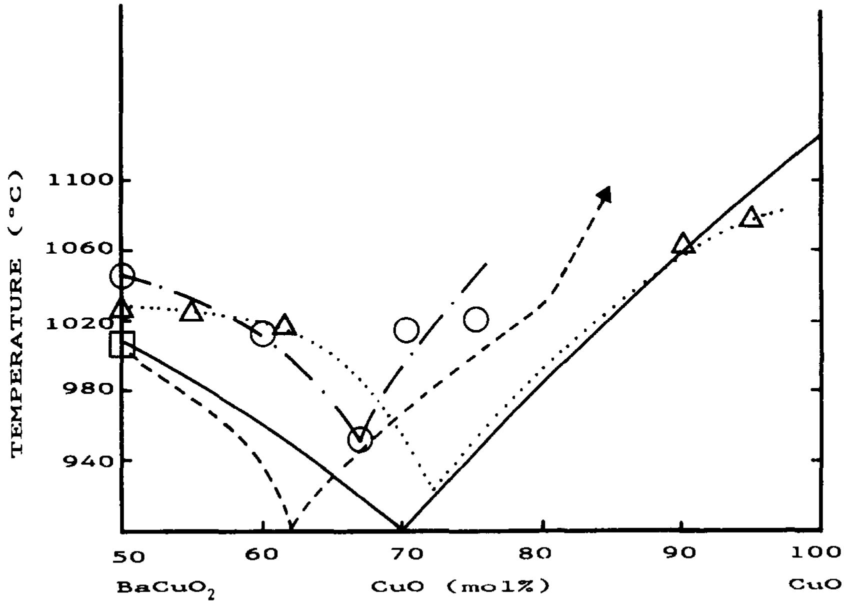

Fig. 1. $BaCuO_2$–CuO phase diagram in air according to literature data — — —, ref. 3; ······, ref. 11; ·—·—·, ref. 15, and calculated by the present authors (———) assuming ideal solution behaviour.

DTA experiments indicate lower melting eutectics at 920 °C and 830 °C in oxygen, and a broad reaction above 918 °C and a well-defined reaction at 818° ± 10 °C in air. This is caused by the additional presence of non-equilibrium phases, as discussed in the following sections. The $BaCuO_2$–CuO system in air is shown, along with the earlier phase diagrams [3,11,15], in Fig. 1. The tentative diagram [20] is based on the above eutectic data, the melting points of $BaCuO_2$ at 1007 °C [21] and of CuO_x at 1130 °C [17], and liquidus curves calculated for ideal-solution behaviour. One might expect a deviation from this ideal behaviour towards complex/compound formation, with consequences on the liquidus curves. The reduction of CuO and $BaCuO_2$ will also be recognized in a final phase diagram which still has to be established.

Crystal growth experiments on YBCO utilizing a solvent of the composition 28 mol% BaO/72 mol% CuO yielded as a secondary crystallization product either CuO [14] or $BaCuO_2$ [22]. This indicates that the ternary eutectic of YBCO, $BaCuO_2$ and CuO lies near the binary eutectic $BaCuO_2$/CuO, and that it is shifted to the CuO-rich side as shown by the point e_1 of Fig. 5 in ref. 17. Depending on the final cooling history of the above crystal growth experiment, even three phases (YBCO, $BaCuO_2$, CuO) could be crystallized before solidification. However, only one or two phases crystallizing above the eutectic temperature would be allowed in equilibrium. A further discussion of this system can be found in ref. 20.

THE SYSTEM YBCO-CuO$_x$

Two groups of researchers indicated that the primary crystallization field of YBCO passed over the connection line YBCO–CuO$_x$ [3,23]. In the hope of finding the possibility of crystallizing YBCO from a Ba-free non-corrosive solvent, a systematic study of the system YBCO–CuO$_x$ was undertaken [24]. In the course of this work we learned about the difficulties of phase-diagram determination in this system, and recognized the non-reproducibility of successive DTA runs in air as shown in Fig. 2. The equilibrium reactions in the first heating curve are subsequently weakened as the non-equilibrium reactions at 782° C, 903° C and 831° C appear. Only after three to five DTA runs is a steady-state situation established, with complex melting and solidification reactions of the equilibrium phases (YBCO, CuO, Y_2BaCuO_5) with non-equilibrium liquid and solid phases (Cu_2O, $BaCuO_2$, Y_2BaCuO_5 at low temperature, and unidentified phases). Figure 3 shows a tentative YBCO–CuO$_x$ phase diagram in oxygen, where the reactions below 1100° C have been established [24]. The high-temperature data and the formation of

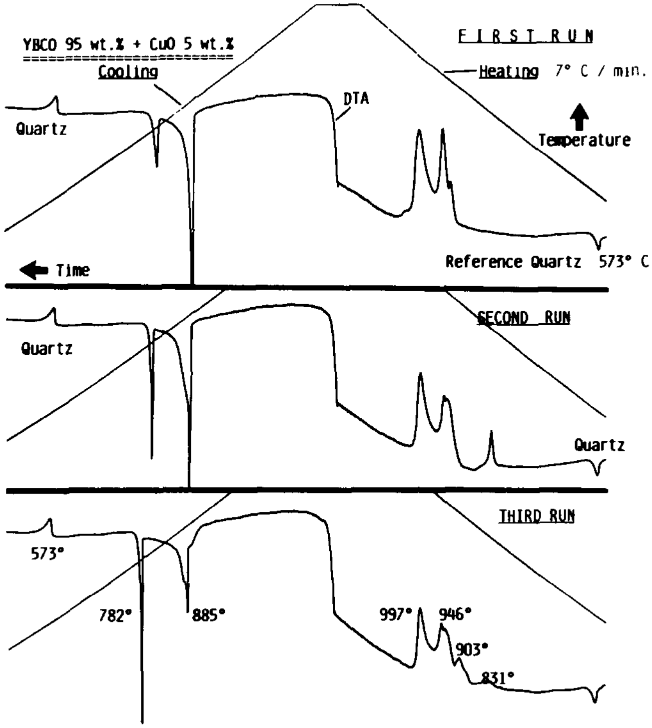

Fig. 2. Successive DTA runs of the 95 wt.% YBCO/5 wt.% CuO composition showing non-equilibrium reactions at around 831° C and 903° C in the second and third heating curves, and at around 782° C in all cooling curves.

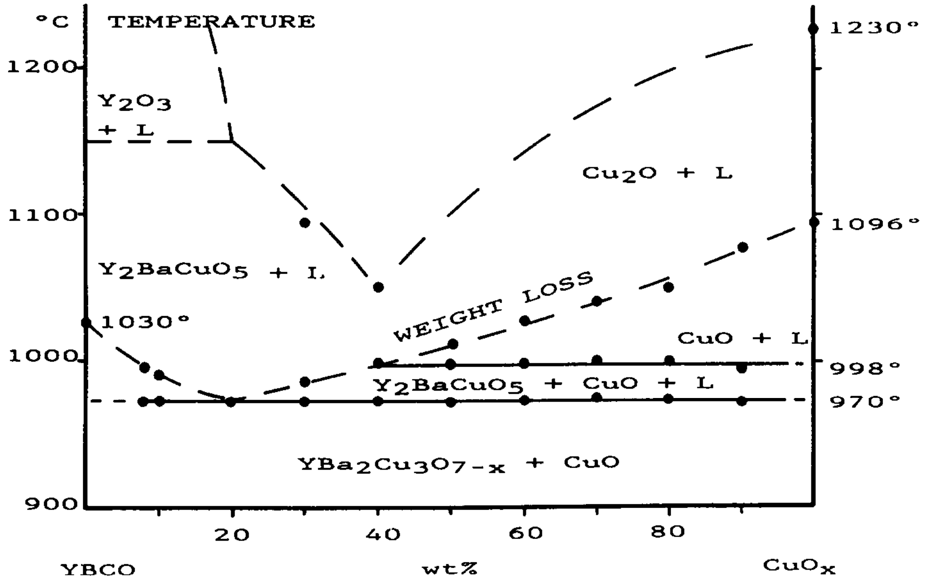

Fig. 3. Tentative YBCO–CuO_x phase diagram in oxygen [24].

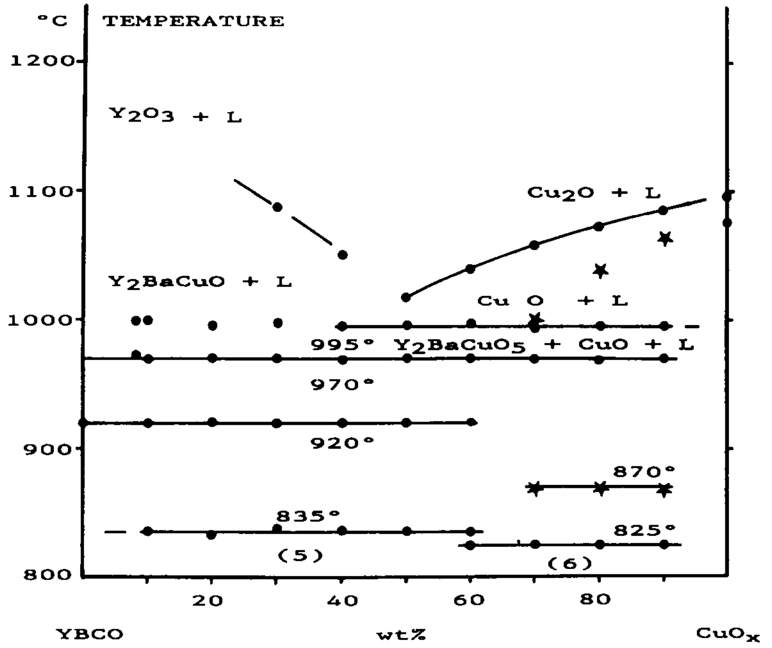

Fig. 4. Non-equilibrium phase diagram of YBCO–CuO_x in oxygen [24] showing additional reactions below 970 °C.

Y_2O_3 are adapted from ref. 17. The corresponding diagram in air is quite similar except for the melting reactions occurring at about 30 °C lower temperatures. A non-equilibrium phase diagram in an oxygen atmosphere is shown in Fig. 4. Owing to only partial reversibility of the reactions

$$\mathrm{YBCO} \rightleftharpoons Y_2BaCuO_5 + \text{liquid} + \text{oxygen} \tag{1}$$

and

$$CuO \rightleftharpoons Cu_2O + \text{oxygen} \tag{2}$$

several low-temperature reactions occur, for instance at 920 °C, 870 °C, 835 °C and 825 °C. The reactions marked by asterisks in Fig. 4 occur when the maximum temperature of 1100 °C has once been surpassed. X-ray analysis of the solidified melt indicated five to six crystalline identified phases and lines of unidentified phase(s), instead of the two equilibrium phases YBCO + CuO.

Concluding this section, it can be said that CuO cannot be used as a solvent for the crystal growth of YBCO. Another feature is the reaction of CuO with YBCO at relatively low temperatures (about 935 °C in air and about 970 °C in oxygen), so that these temperatures should not be exceeded when fabricating YBCO ceramics with excess CuO: Y_2BaCuO_5 otherwise may be formed as a relatively stable secondary phase with a detrimental effect on superconducting transport properties.

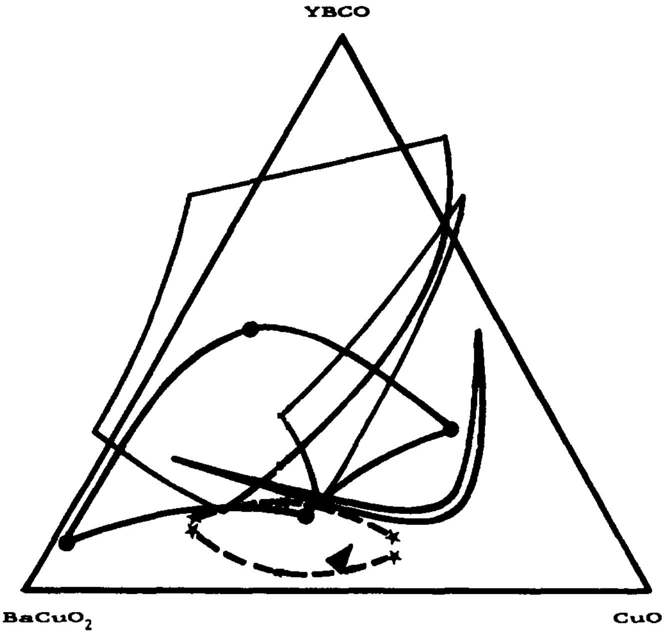

Fig. 5. The primary crystallization fields of YBCO in the pseudo-ternary system BaO–CuO–Y_2O_3, shown for the section $BaCuO_2$–CuO–YBCO, according to different authors [3,17,19,21,23,30] (in molar composition).

THE SYSTEM Y_2O_3–BaO–CuO

This system was not investigated before 1987 and is not listed in phase diagram compilations (Phase Diagrams for Ceramists, etc.). Shortly after the discovery of high-temperature superconductivity above liquid-nitrogen temperatures by Wu et al. [25], and after the identification and structure determination of the superconducting phase $YBa_2Cu_3O_7$ by various research groups, preliminary investigations of the ternary phase diagram were undertaken. First, the sub-solidus phase coexistence fields were established [26–29]. Of interest for crystal growers specifically is the primary crystallization field (PCF) of YBCO. Publications of various research groups [3,17,19,21,23,30] show large differences in the size and position of this PCF, as shown in Fig. 5. Perhaps these differences result from difficulties in phase diagram determination as indicated in the above sections. Different methods (DTA, TG, annealing/quenching experiments and crystal growth experiments) and different parameters (heating/cooling rates, oxygen partial pressure and crucible material) may explain the wide scatter of published PCFs. The

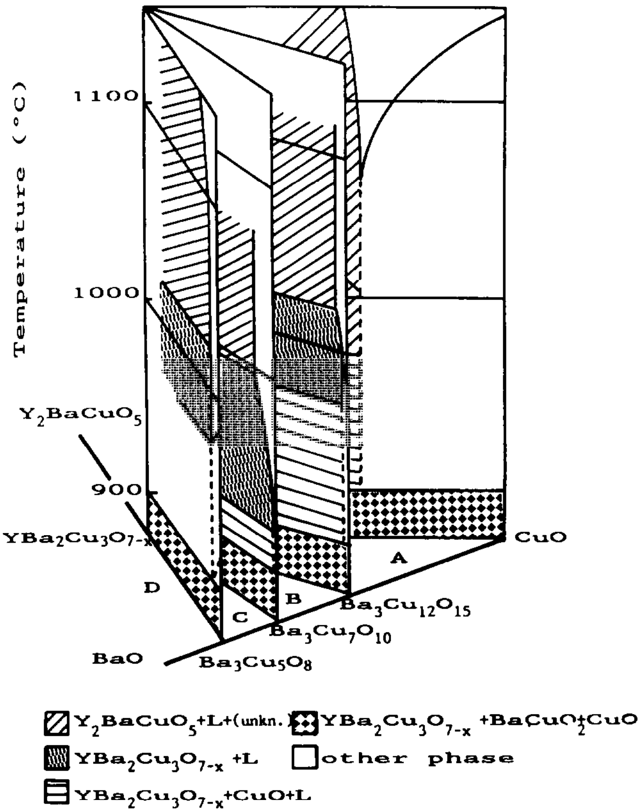

Fig. 6. Phase relation of YBCO with different BaO/CuO ratios [19].

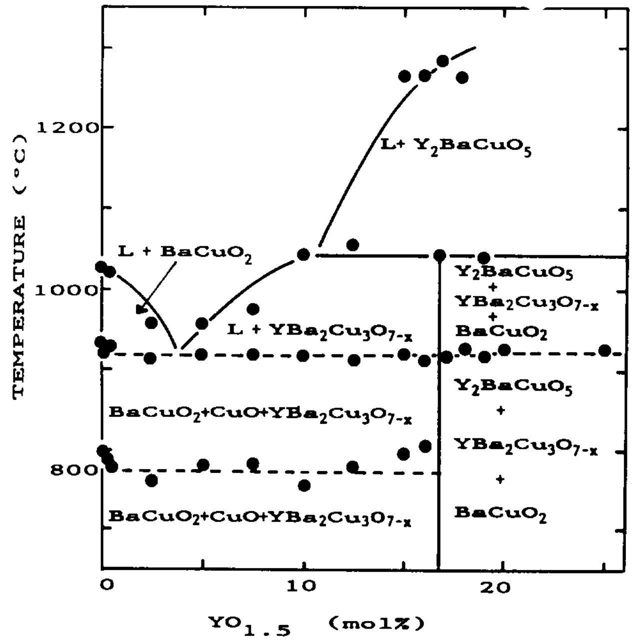

Fig. 7. Pseudobinary section of YBCO–33.3 mol% BaO/66.7 mol% CuO phase diagram in oxygen, from ref. 15.

present authors have begun to investigate a few sections of the ternary phase diagram in order to determine the widths and positions of the PCF for optimization of crystal growth conditions and for achieving liquid-phase epitaxy. As a first working hypothesis, a PCF between those of ref. 19 and ref. 21 is assumed. In the systematic work of Oka et al. [19] three sections of different BaO–CuO compositions with YBCO were analyzed, and the crystallization range of YBCO was established. Their composite presentation of the phase relation is shown in Fig. 6. They used tiny Pt crucibles with samples of weight 20–30 mg and applied heating/cooling rates of 10 °C min^{-1}; their data do not indicate interference from platinum corrosion and Pt-containing compounds. From the data given for the BaO–CuO-rich side, one could deduce the eutectic temperature of the system BaCuO$_2$–CuO at 910–920 °C and the eutectic composition at 30 mol% BaO, thus confirming the conclusions drawn above for BaO–CuO$_x$. One pseudobinary section of YBCO-33.3 mol% BaO/66.7 mol% CuO in oxygen obtained by Nomura et al. [15] is shown in Fig. 7. The temperatures are generally about 20 °C higher than our data and most of the published data. Also the melting point of the BaO/CuO solvent is too high; perhaps the melting point of pure BaCuO$_2$ had been used to design the figure. Otherwise this diagram is quite similar to the data in ref. 17 and to our data which are to be published. Nomura et al. [15] claim the stability of an orthorhomic YBCO in an Y$_2$O$_3$-rich environment in an oxygen atmosphere up to about 920 °C; however, this requires

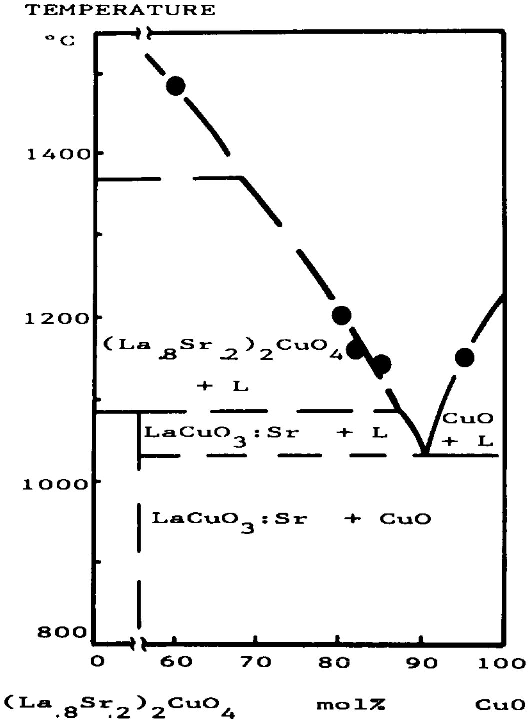

Fig. 8. $(La,Sr)_2CuO_4$–CuO phase diagram with literature data [49,62], from ref. 58.

further investigation. On the other hand, in solidified melts on the BaO–2CuO-side, the orthorhombic–tetragonal transition lies in the usual 750 °C region. The effect of oxygen partial pressure on the stability range of YBCO and on the tetragonal–orthorhombic phase transition will not be reviewed here; references are merely given [31–34].

The discussion on PCFs indicated already that YBCO does not melt congruently. By heating to 1000 ± 3 °C in air and to 1028 ± 3 °C in oxygen, YBCO decomposes into the "green phase" Y_2BaCuO_5 + liquid. This reaction and these temperatures are found by most groups. According to Roth et al. [21] there are no further reactions (except for some uptake of CO_2) until the liquidus point is reached. According to ref. 17 a sample of $YBa_2Cu_3O_7$ heated to 1300 °C contains Y_2O_3 + liquid, indicating a decomposition of the green phase before the liquidus point is reached. The nature of the primary crystallization product on cooling an oxide melt of the cation ratio 1Y : 2Ba : 3Cu, "123" may become important for melt processing of YBCO. Therefore, an experiment was performed to heat a pellet of the 123 composition at 1300 °C for 2 h and to air-quench the melt: the presence of Y_2O_3 in the X-ray pattern indicates that the PCF of Y_2O_3 extends to the YBCO 123 composition.

The effect of CO_2 on the phase diagram and on the existence and melting behaviour of specific phases has been postulated [21] but not substantiated by direct evidence (for instance by quantitative analysis of CO_2 by dissolving Y–Ba–Cu–O oxides in acids). A possible alternative explanation of the observed effects could be the loss of oxygen at high temperatures: this leads to the formation of reduced solid and liquid non-equilibrium phases, to new phases, and to low-temperature (below 900 ° C) complex melting reactions (see the section on YBCO–CuO).

No solid solubility of YBCO with one of the constituent oxides could so far be detected. The first indication of this fact by Hinks et al. [35] was confirmed by other research groups [36,37]. The extremely small solid solubility of YBCO causes difficulties in preparation of stoichiometric YBCO ceramics [38], since the smallest deviation from stoichiometry or any inhomogeneity leads to the formation of secondary phases. This obviously is detrimental for the superconducting properties, especially the critical current density [38]. A simple method for detection of traces of secondary phases [10] allows development of YBCO ceramics with less than 0.5 wt.% of secondary phases having improved critical current densities [39]. The negligible solid solubility also has advantages, for instance in crystal growth, where stoichiometric YBCO crystals are obtained automatically from high-temperature solutions [40].

For further presentations of pseudobinary systems involving YBCO, it is suggested to use wt.% YBCO because the molecular weights of fluxes can be misinterpreted.

YBCO CRYSTAL GROWTH AND CRYSTAL SEPARATION

The lack of phase diagram data inhibited crystal growth in the initial phase after discovery of high-temperature superconductivity. Small crystals obtained in solid-state reactions, perhaps with the help of transient liquid phases, were useful for structure determination. Crystals of YBCO were then obtained in solidified non-stoichiometric melts using excess BaO–CuO. These crystals, of limited size, were recovered partially from cavities formed during the solidification process (cavity method), and partially by mechanical separation by means of a dentist's drill machine from the solidified mass. These early crystals obtained by several research groups [9,14,23,41–53] were important for initial physical measurements.

The first separation of YBCO crystals after growth from the still liquid flux was achieved by Scheel and Licci and was reported at the MRS Fall Meeting 1987 at Boston [54]. This result was achieved owing to initial knowledge of a primary crystallization field of YBCO [55]. Larger crystals could then be grown from high-temperature solutions [1] and separated from the flux by decanting [22] and by suction using a ceramic plug [56]. The crystal growth problems and results have been reviewed recently and will not be further discussed here [40,57,58].

$La_{1.85}Sr_{0.15}CuO_4$: PHASE DIAGRAM AND CRYSTAL GROWTH

Based on the discovery of high-temperature superconductivity in the La–Ba–Cu–O system by Bednorz and Müller [59], the compound $La_{1.85}Sr_{0.15}CuO_4$, "LASCO", having slightly higher T_c of above 40 K was discovered [60,61]. Figure 8 shows the phase diagram $(La,Sr)_2CuO_4$–CuO using data from Hidaka et al. [49] and Chen et al. [62]. It indicates that LASCO melts incongruently and thus cannot be directly grown from melts. However, its thermal stability to nearly 1400 ° C allows use of excess CuO as solvent to grow LASCO from relatively concentrated (15–30 mol%) high-temperature solutions. Various research groups [49,62–64] have grown crystals of LASCO mainly by top-seeded solution growth and by the floating-crystal technique. Difficulties encountered are sufficiently high Sr-concentration for high T_c, growth instability, and cracking. Further studies of the phase diagram of this system have been published in refs. 65 to 67.

Bi- AND Tl-CUPRATE PHASES

After the discovery of superconductivity above 100 K in the Bi–Ca–Sr–Cu–O and Tl–Ba–Ca–Cu–O phases, numerous attempts at crystal growth were performed [68–81] without any knowledge of the phase relations. In most cases, different ratios of the constituent oxides and excess CuO were partially or completely melted, and crystallization was induced by slow cooling. Also the low-melting eutectic [82] of 90 mol% Bi_2O_3/10 mol% CuO ($T_{eut.} \approx 600\,^\circ C$) was used for crystallizing Bi-cuprate phases [75]. Usually, very thin plates of a few millimetres lateral dimensions were obtained in the solidified mass. Mechanical separation has limited so far the size of the "free" crystals. These crystals generally are not single phase, as they contain stacks of various layer compounds, a case of "chemical polytypism".

Alternative attempts at crystal growth were carried out using the "travelling solvent float zone" [79] and the Bridgman methods [72]. Schneemeyer et al. [70] and Katsui [73] used KCl, and alkali chlorides in general, as high-temperature solvents for Bi-cuprates: advantages were reduced corrosion of (Pt) crucibles and crystal separation by dissolving the flux in water. First attempts at liquid-phase epitaxy from either non-stoichiometric melts [83,84] or from alkali halide solvents [85] have been reported.

CONCLUSIONS

Knowledge of the specific phase diagrams can be summarized as follows. The system $(La_{1-x}Sr_x)_2CuO_4$ is reasonably well understood, and allows growth of relatively large crystals. The system YBCO–$BaCuO_2$–CuO is only partially understood; the primary crystallization field of YBCO and its liquidus surface especially need to be determined. The eutectic compositions and temperatures for the binary system $BaCuO_2$–CuO in air and in oxygen need to be confirmed and the actual liquidus temperatures determined. The ternary eutectic of the system YBCO–$BaCuO_2$–CuO should be established in order to find the lowest melt-assisted preparation temperature for YBCO.

Practically no phase data exist for the Bi- and Tl-based cuprate superconductors. Congruent or incongruent melting behaviour of some of these compounds in the temperature range 850°C to 930°C merely were reported. Large, free and structurally pure crystals of these interesting compounds have not been achieved as yet.

The slow progress in knowledge of the phase diagrams of the new superconductors hampers the synthesis of high-purity compounds and significant developments in crystal growth and epitaxy. Mastering the materials problems is necessary also for applications of HTSC in the form of thin films and of polycrystalline wires and tapes. The difficulties in the phase studies result from the complexity and from unforeseen difficulties as explained in the above section on experimental aspects and problems. The pace of careful phase-diagram determination could not in any case follow the rapid developments and discoveries of HTSC compounds, so that work in one typical system may be "out of date" when HTSC compounds with improved T_c and properties are found.

Sufficient knowledge of the phase relations of high-temperature superconductors should be supplemented by physico-chemical studies of melts and solutions and by determination of the thermodynamic data of compounds and reactions. These experimental results could then be utilized for a "full" theoretical description of the phase relations of the cuprate superconductors: a challenge for years to come.

REFERENCES

1 D. Elwell and H.J. Scheel, Crystal Growth from High Temperature Solutions, Academic Press, London, 1975, Chaps. 6 and 7.
2 D. Rytz and H.J. Scheel, J. Cryst. Growth, 59 (1982) 468.
3 R.S. Roth, K.L. Davis and J.R. Dennis, Adv. Ceram. Mater., 2 (1987) 303.
4 Y. Laligant, G. Ferey, M. Hervieu and B. Raveau, Europhys. Lett., 4 (1987) 1023.
5 G. Calestani, C. Rizzoli and G.D. Andreetti, Solid State Commun., 66 (1988) 223.
6 F. Licci, H.J. Scheel and J. Sommerauer, unpublished.
7 H.J. Scheel, W. Sadowski and L. Schellenberg, Supercond. Sci. Technol. 2 (1989) 17.

8 Th. Wolf, W. Goldacker, B. Obst., G. Roth and R. Flükiger, J. Cryst. Growth 96 (1989) 1010.

9 L.F. Schneemeyer, J.W. Waszczak, T. Siegrist, R.B. van Dover, L.W. Rupp, B. Batlogg, R.J. Cava and D.W. Murphy, Nature, 328 (1987) 601.

10 M. François and H.J. Scheel, J. Less-Common Met., 150 (1989) 211.

11 M. Nevřiva, E. Pollert, L. Matějková and A. Tříska, J. Cryst. Growth, 91 (1988) 434.

12 A.B. Bykov, L.N. Demianets, I.P. Zibrov, G.V. Kanunnikov, O.K. Melnikov and S.M. Stishov, J. Cryst. Growth, 91 (1988) 302.

13 J. Wojcik, M. Rosochowska, H. Niculescu and A. Pajaczkowska, J. Cryst. Growth, 91 (1988) 255.

14 G. Balestrino, S. Barbanera and P. Paroli, J. Cryst. Growth, 85 (1987) 585.

15 S. Nomura, H. Yoshino and K. Ando, J. Cryst. Growth, 92 (1988) 682.

16 F. Greuter, P. Kluge-Weiss, H. Zimmermann and C. Schüler, Physica C, 153–155 (1988) 361.

17 T. Aselage and K. Keefer, J. Mater. Res., 3 (1988) 1279.

18 D.M. de Leeuw, C.A.H.A. Mutsaers, C. Langereis, H.C.A. Smoorenburg and P.J. Rommers, Physica C, 152 (1988) 39.

19 K. Oka, K. Nakane, M. Ito, M. Saito and H. Unoki, Jpn. J. Appl. Phys., 27 (1988) L1065.

20 F. Licci, H.J. Scheel and P. Tissot, in preparation.

21 R.S. Roth, C.J. Rawn, F. Beech, J.D. Whitler and J.O. Anderson, in M.F. Yan (Ed.) Ceramic Superconductors II, American Ceramics Society, Westerville, 1988, p. 13.

22 W. Sadowski and H.J. Scheel, J. Less-Common Met., 150 (1989), 219.

23 S. Takekawa and N. Iyi, Jpn. J. Appl. Phys., 26 (1987) L851.

24 F. Licci, P. Tissot and H.J. Scheel, J. Less-Common Met., 150 (1989) 201.

25 M.K. Wu, J.R. Ashburn, C.J. Torng, P.H. Hor, R.L. Meng, L. Gao, Z.J. Huang, Y.Q. Wang and C.W. Chu, Phys. Rev. Lett., 58 (1987) 908.

26 K.J. Frase, E.G. Liniger and D.R. Clarke, J. Am. Ceram. Soc., 70 (1987) C-204.

27 G. Wang, S.-J. Hwu, S.N. Song, J.B. Ketterson, L.D. Marks, K.R. Poeppelmeier and T.O. Mason, Adv. Ceram. Mater., 2 (1987) 313.

28 L.P. Cook, C.K. Chiang, W. Wong-Ng and J. Blendel, Adv. Ceram. Mater., 2 (1987) 656.

29 K.G. Frase and D.R. Clarke, Adv. Ceram. Mater., 2 (1987) 295.

30 K. Fischer, R. Hergt and D. Linzen, Cryst. Res. Technol., 23 (1988) 1169.

31 P.K. Gallagher, Adv. Ceram. Mater., 2 (1987) 632.

32 H.M. O'Bryan and P.K. Gallagher, Adv. Ceram. Mater., 2 (1987) 640.

33 B.T. Ahn, T.M. Gür, R.A. Huggins, Physica C, 153–155 (1988) 590.

34 J. Karpinski, E. Kaldis and S. Rusiecki, J. Less-Common Met., 150 (1989) 207.

35 D.G. Hinks, L. Soderholm, D.W. Capone, J.D. Jorgensen, I.K. Schuller, C.U. Serge, K. Zhang and J.D. Grace, Appl. Phys. Lett., 50 (1987) 1688.

36 G.R. Wagner, A.J. Panson and A.I. Braginski, Phys. Rev. B, 36 (1987) 7124.

37 T. Graf, J.L. Jorda and J. Muller, J. Less-Common Met., 146 (1989) 49.

38 H.J. Scheel, F. Licci, T. Besagni, F. Bolzoni, S. Cattani, D. Eckert and G. Salviati, Mater. Science Eng. A109 (1988) 299.

39 H.J. Scheel, D. Cattani, D. Eckert, F. Licci and T. Besagni, unpublished.

40 H.J. Scheel, J. Less-Common Met., 151 (1989) 199.

41 J.Z. Liu, G.W. Crabtree, A. Umezawa and Li Zongquan, Phys. Lett. A, 121 (1987) 305.

42 Y. Oda, T. Kohara, I. Nakada, H. Fujita, T. Kaneko, H. Toyoda, E. Sakagami and K. Asayama, Jpn. J. Appl. Phys., 26 (1987) L809.

43 T.R. Dinger, T.K. Worthington, W.J. Gallagher and R.L. Sandstrom, Phys. Rev. Lett., 58 (1987) 2687.

44 S. Hayashi, H. Komatsu, T. Inoue, T. Ono, K. Sasaki, J. Koike and T. Fukase, Jpn. J. Appl. Phys., 26 (1987) L1197.

45 M.A. Damento, K.A. Gschneidner, Jr., and R.W. McCallum, Appl. Phys. Lett., 51 (1987) 690.

46 D.L. Kaiser, F. Holtzberg, B.A. Scott and T.R. McGuire, Appl. Phys. Lett., 51 (1987) 1040.

47 H. Takei, H. Takeya, Y. Iye, T. Tamegai and F. Sakai, Jpn. J. Appl. Phys., 26 (1987) L1425.

48 A. Katsui, Y. Hidaka and H. Ohtsuka, Jpn. J. Appl. Phys., 26 (1987) L1521.

49 Y. Hidaka, Y. Enomoto, M. Suzuki, M. Oda and T. Murakami, J. Cryst. Growth, 85 (1987) 581.

50 B.N. Das, L.E. Toth, A.K. Singh, B. Bender, M. Osofsky, C.S. Pande, N.C. Koon and S. Wolf, J. Cryst. Growth, 85 (1987) 588.

51 D.L. Kaiser, F. Holtzberg, M.F. Chisholm and T.K. Worthington, J. Cryst. Growth, 85 (1987) 593.

52 H.J. Scheel and F. Licci, J. Cryst. Growth, 85 (1987) 607.

53 H. Katayama-Yoshida, Y. Okabe, T. Takahashi, T. Sasaki, T. Hirooka, T. Suzuki, T. Ciszek and S.K. Deb, Jpn. J. Appl. Phys., 26 (1987) L2007.

54 H.J. Scheel and F. Licci, MRS Proc., 99 (1988) 595.

55 F. Licci, H.J. Scheel and T. Besagni, Physica C, 153–155 (1988) 431.

56 R. Boutellier, B.N. Sun, H.J. Scheel and H. Schmid, J. Cryst. Growth, 96 (1989) 465.

57 H.J. Scheel, Physica C, 153–155 (1988) 44.

58 H.J. Scheel and F. Licci, Mater. Res. Bull., 13 (10) (1988) 56.

59 J.G. Bednorz and K.A. Müller, Z. Phys. B, 64 (1986) 189.

60 R.J. Cava, R.B. van Dover, B. Batlogg and E.A. Rietman, Phys. Rev. Lett., 58 (1987) 408.

61 K. Kishio, K. Kitazawa, S. Kanbe, I. Yasuda, N. Sugai, H. Takagi, S. Uchida, K. Fueki and S. Tanaka, Chem. Lett., (1987) 429.

62 C. Chen, B.E. Watts, B.M. Wanklyn, P.A. Thomas and P.W. Haycock, J. Cryst. Growth, 91 (1988) 659.

63 P.J. Picone, H.P. Jenssen and D.R. Gabbe, J. Cryst. Growth, 85 (1987) 576.

64 K. Oka and H. Unoki, Jpn. J. Appl. Phys., 26 (1987) L1590.

65 L.R. Morss, D.C. Sonnenberger and R.J. Thorn, MRS Proc., 99 (1988) 571.

66 C. Chen, B.E. Watts, B.M. Wanklyn and P. Thomas, Solid State Commun., 66 (1988) 611.

67 P.J. Picone, H.P. Jenssen and D.R. Gabbe, J. Cryst. Growth, 91 (1988) 463.

68 J.Z. Liu, G.W. Crabtree, L.E. Rehn, Urs Geiser, D.A. Young, W.K. Kwok, P.M. Baldo, J.M. Williams and D.J. Lam, Phys. Lett. A, 127 (1988) 444.

69 Y. Hidaka, M. Oda, M. Suzuki, Y. Maeda, Y. Enomoto and T. Murakami, Jpn. J. Appl. Phys., 27 (1988) L538.

70 L.F. Schneemeyer, R.B. van Dover, S.H. Glarum, S.A. Sunshine, R.M. Fleming, B. Batlogg, T. Siegrist, J.H. Marshall, J.W. Waszczak and L.W. Rupp, Nature, 332 (1988) 422.

71 Y. Koike, T. Nakanomoyo and T. Fukase, Jpn. J. Appl. Phys., 27 (1988) L841.

72 A. Ono, S. Sueno and F.P. Okamura, Jpn. J. Appl. Phys., 27 (1988) L786.

73 A. Katsui, Jpn. J. Appl. Phys., 27 (1988) L844.

74 B. Morosin, D.S. Ginley, E.L. Venturini, P.F. Hlava, R.J. Baughman, J.F. Kwak and J.E. Schirber, Physica C, 152 (1988) 223.

75 P.A. Morris, W.A. Bonner, B.G. Bagley, G.W. Hull, N.G. Stoffel, L.H. Greene, B. Meagher and M. Giroud, Appl. Phys. Lett., 53 (1988) 249.

76 D.S. Ginley, B. Morosin, R.J. Baughman, E.L. Venturini, J.E. Schirber and J.F. Kwak, J. Cryst. Growth, 91 (1988) 456.

77 S. Nomura, T. Yamashita, H. Yoshino and K. Ando, Jpn. J. Appl. Phys., 27 (1988) L1251.

78 Z. Ren, X. Yan, Y. Jiang and W. Guan, J. Cryst. Growth, 92 (1988) 677.

79 S. Takekawa, H. Nozaki, A. Umezono, K. Kosuda and M. Kobayashi, J. Cryst. Growth, 92 (1988) 687.

80 G. Balestrino, U. Gambardella, Y.L. Liu, M. Marinelli, A. Paoletti, P. Paroli and G. Paterno, J. Cryst. Growth, 92 (1988) 674.

81 J.-M. Imer, F. Patthey, B. Dardel, W.-D. Schneider, Y. Bear, Y. Petroff and A. Zettl, Phys. Rev. Lett., 62 (1989) 336.

82 E.M. Levin and H.F. McMurdie, Phase Diagrams for Ceramists, The American Ceramics Society, Columbus, OH, 1975, Fig. 4178.

83 R.S. Liu, Y.T. Huang, P.T. Wu and J.J. Chu, Jpn. J. Appl. Phys., 27 (1988) L1470, and Physica C 156 (1988) 197.

84 R.S. Liu, Y.T. Huang, J.M. Liang and P.T. Wu, Physica C, 156 (1988) 785.

85 G. Balestrino, A. Paoletti, P. Paroli and P. Romano, Appl. Phys. Lett. 54 (1989) 2041.